The Journal of Engineering

The 9th International Conference on Power Electronics, Machines and Drives (PEMD 2018)

IET Journals
The Institution of Engineering and Technology

Novel maximum power point tracking strategies for electronically tuned linear alternators

eISSN 2051-3305
Received on 22nd June 2018
Accepted on 27th July 2018
E-First on 4th June 2019
doi: 10.1049/joe.2018.8089
www.ietdl.org

Min Zhang[1] ✉, *Matteo F. Iacchetti*[1], *Roger Shuttleworth*[1]

[1]*School of Electrical and Electronic Engineering, The University of Manchester, Manchester, M13 9PL, UK*

✉ *E-mail: min.zhang-5@student.manchester.ac.uk*

Abstract: Linear alternators (LAs) are widely applied in many energy conversion systems based on pressure waves, to avoid linear to rotary conversion mechanisms. The control of the LA is the key element to maximise the system's electric power and efficiency. However, the LA resonant frequency cannot be accurately controlled by mechanical design due to parameter tolerance. Furthermore, the operating frequency is generally not strictly constant in real-time, making maximum power point tracking (MPPT) hard to achieve. Two MPPT strategies are proposed here to adjust the electronic stiffness amount in real time. They are hereafter referred to as symmetrical signal injection method and electronic stiffness perturbation method. The latter one is selected and validated via simulation studies.

1 Introduction

LAs have been used in various applications such as thermo-acoustic engines (TAEs), free-piston stirling engines (FPSEs), and direct-drive wave energy converters (DD-WECs). Existing control techniques dealing with control of LA are mainly focussing on DD-WECs [1–4]. Only a few LA control strategies are proposed for TAE and FPSE applications [5]. The LA resonant frequency needs to be accurately matched with the frequency of the driving force. However, in practical applications, the operation frequency is prone to drift. Also, the LA resonant frequency is generally calculated by spring stiffness and mass. However, parasitic effects such as the cogging force, change the resonance frequency, especially for moving-magnet topologies [6]. Furthermore, LAs usually need to be sealed in a vessel due to harsh working environment. The bounce space contributes to the overall stiffness. Therefore, overall stiffness composes of mechanical spring stiffness, bounce space stiffness, and cogging force equivalent stiffness.

The resonant frequency matching requirement cannot in general be met by relying only on mechanical design of the LA, but this can be achieved with the help of the power electronic interface. Several papers relevant to DD-WEC have addressed the electronic stiffness regulation by using VSI [1, 3, 4]. Several reaction force stiffness regulation schemes are proposed in [2–4] to achieve resonant tuning with phase and amplitude controllers for LA currents. A reactive current is injected by the inverter to create some 'electronic stiffness' and adjust the overall stiffness. However, these controls are all based on accurate WEC system model and accurate knowledge of the system parameters [2].

A maximum power point tracking (MPPT) control scheme is proposed in [1] to ensure the excitation force which is in phase with the velocity. However, the velocity and acceleration information are required to estimate the wave period [1]. A MPPT technique is proposed in WEC [7] to avoid using position information. The strategy compares the current output power of WEC with the output power from the previous time interval to identify control direction. However, the time interval is hard to obtain accurately especially for the irregular period wave actuation source. To improve the control accuracy, zero crossing detection strategy is compulsory to use, which is generally sensitive to signal interference and DC bias. Finally, even if the existing techniques can to some extent achieve mechanical resonance conditions for the LA, they do not take into account the equivalent mechanical impedance of the source and then cannot guarantee the optimal impedance matching for the full system including the power source.

Within existing MPPT strategies developed for LA, the signal injection method has not be employed yet. With small-signal injection, information can be extracted from either stroke or output power. The signal injection control schemes can be implemented without relying on accurate system model and measurement of the LA parameters. Here, two MPPT strategies are proposed to adjust the electronic stiffness in real time, to automatically maximise the system power output without relying on knowledge of LA parameters. The first one is the symmetrical signal injection method. Two small current signals are injected into VSI with frequency set to be symmetrically above and below the operating frequency. The corresponding stroke components are tracked to identify the resonance condition on the basis of the symmetry in their phase shifts. The second method is an electronic stiffness perturbation method. A small perturbation current signal is injected into the LA and extracted information from output DC power is used to control. The second method is easier to implement and is then validated with a simulation study.

2 Background

The LA-VSI layout is shown in Fig. 1. A moving magnet LA is coupled to a back to back VSI power electronic interface. The left VSI is work in regenerative mode in order to control the LA. The DC output of the left VSI is stabilised with the help of the DC link capacitor and right side VSI. Also, the right side VSI will convert the DC to AC output which may fit to the mains. The piston coupled to LA shaft is pushed by a reciprocating source force $F(t)$.

The equivalent circuit for LA-VSI is shown in Fig. 2. The mass of LA moving carriage, equivalent stiffness, and damping is expressed in m, k and c. The source force is described in phasor $\bar{F}$. An electromagnetic force $\bar{F}_e$ is produced onto the moving carriage. An emf $\bar{E}$ is induced on the coil and the back-EMF constant is expressed in k_e. Parameters L and R refer to the coil inductance and resistance. The linear alternator (LAs) is fed by VSI with a fast current control loop. The actual stator current tracks the reference current value provided by the controller. The control of the second VSI is well documented in literature and is not the main task for this study, so it is replaced by a DC voltage source V_{dc}.

The steady-state operation frequency of the source force is expressed as ω_o. The stroke of the LA is denoted by x. The steady-state relations can be described in terms of phasors by

$$(-\omega_o^2 m + j\omega_o c + k)\bar{x} = \bar{F} - k_e\bar{I} \quad (1)$$

$$\bar{E} = j\omega_o k_e \bar{x} \quad (2)$$

$$\bar{V} = \bar{E} - R\bar{I} - j\omega_o L\bar{I} \quad (3)$$

Corresponding to (1)–(3), the phasor diagram for the maximum power extraction condition is shown in Fig. 3.

For the reference frame dq: the d-axis is parallel to the stroke phasor $\bar{x}$ and the q-axis is in quadrature to the stroke. In resonant condition, the equivalent stiffness force term kx and inertia term $-\omega_o^2 mx$ should cancel each other. By controlling armature current in quadrature with stroke, the resonant frequency of the LA can be adjusted to match with the operating frequency. The resonant frequency of the LA is

$$\omega_n = \sqrt{k/m} \quad (4)$$

Since the q-axis current is response for the active power conversion, the maximum power is obtained in this condition. The generated active power is calculated as

$$P = \omega k_e x I_q \quad (5)$$

In order to understand the effort of the electronic stiffness, two phasor diagrams are presented in Fig. 4 to identify the difference between two conditions: without electronic stiffness (left) and with electronic stiffness (right).

For the comparison, the amplitude and frequency of the source force are assumed to remain the same. The q-axis current is maintained constant at the same value in the two conditions, in order to preserve the in-quadrature component of the electromagnetic force (active component). In Fig. 4*a*, insufficient spring stiffness leads to a mismatch between system frequency and LA resonant frequency which then reduces the stroke below the rated value. The emf as well as extracted power are reduced with the decrease of the stroke. In second case, the armature current phasor is split into two components: d-axis current $\bar{I}_d$ parallel to $\bar{x}$ and q-axis current $\bar{I}_q$ in perpendicular to $\bar{x}$. The in-phase current $\bar{I}_d$ is regulated to produce a stiffness force bringing additional electronic stiffness k_v

$$k_v = k_e I_d / x \quad (6)$$

Generally, the in-quadrature current $\bar{I}_q$ is reduced with increasing of the $\bar{I}_d$ due to the maximum current constraint.

$$I_q = \sqrt{I^2 - I_d^2} = \sqrt{I^2 - (k_v x/k_e)^2} \quad (7)$$

Based on (6), (1) is rewritten into

$$(-\omega_o^2 m + j\omega_o c + k + k_v)\bar{x} = \bar{F} - jk_e\bar{I}_q \quad (8)$$

It is discussed in [8] that the additional d-axis current will require an oversized power electronic design. However, in this study, the impact of electronic stiffness control strategy on the rating of power electronic interface and LA design will not be considered. Conversely, it will be assumed that the LA has a proper design to allow bigger current capability.

3 Symmetrical signal injection method

The symmetrical signal injection algorithm is shown in Fig. 5, to implement the MPPT. A stroke sensor such as linear variable differential transformer (LVDT) will measure the stroke. A phase-lock loop (PLL) control system receives this stroke signal and track for the main harmonic. The PLL either generates an output signal whose phase is tracked with the phase of the input stroke signal or provides an accurate measurement for the main harmonic frequency. The output unit sinusoidal signal is used to produce reference current signals in-phase and in-quadrature to the stroke signal. The required reference d-axis current I_d^* is controlled by MPPT algorithm to adjust the electronic stiffness in real time. The q-axis reference current is set to a fixed value. The error between overall reference current I_{LA}^* and actual current of LA is used by a fast hysteresis comparator to produce PWM signal, which is then used to control the VSI switches. Two small current signals are injected into the LA by the VSI. Their frequency will be set to be symmetrically below or above the operation frequency which is controlled by PLL. These two small current signals will produce a reactive force producing corresponding harmonic components in the stroke and velocity. PLL will not respond to these small signals as their amplitude is far away from the main harmonic. Therefore, the electronic stiffness is only acting on the main stroke harmonic component.

Based on (1), the resulted stroke when the small signal is injected is expressed as

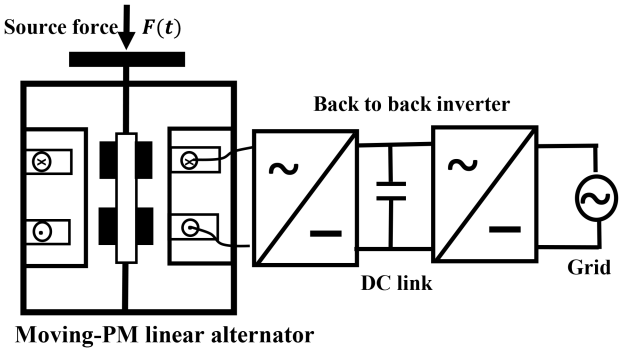

Fig. 1 *Moving-magnet LA coupled with back to back VSI*

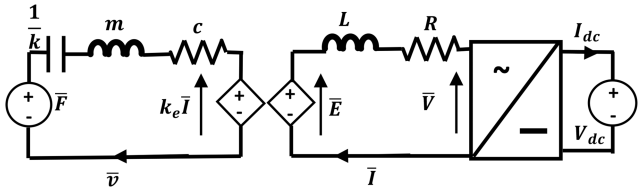

Fig. 2 *Equivalent circuit for LA-VSI system*

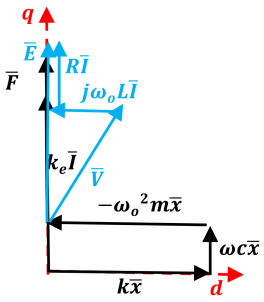

Fig. 3 *Phasor diagram of the LA with VSI being proper controlled (maximum power condition)*

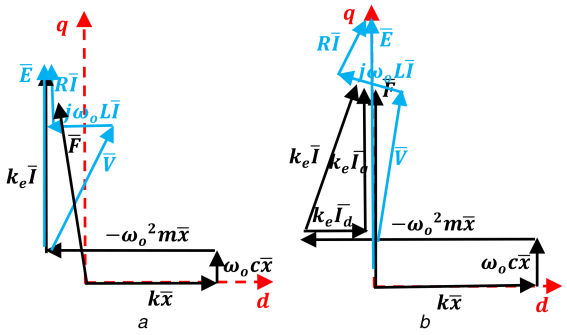

Fig. 4 *Phasor diagram for the LA with VSI being proper controlled*
(a) No electronic stiffness, ***(b)*** With electronic stiffness

$$\bar{x}_{\text{injected}} = \frac{\bar{F}_{\text{injected}}}{(k - \omega_{\text{injected}}^2 m) + j\omega_{\text{injected}} c} \tag{9}$$

The damping ratio is defined as ratio of actual damping and critical damping. It is expressed as

$$\xi = c/c_{\text{cri}} = c/2m\omega_n \tag{10}$$

From (4), (9) and (10), the phase of the stroke is

$$\arg(x) = \arctan\left(\frac{2\zeta(\omega_{\text{injected}}/\omega_n)}{1 - (\omega_{\text{injected}}/\omega_n)^2}\right) \tag{11}$$

It can be found that when the frequency ratio is within a narrow range near unity, the relationship between phase and frequency ratio can be approximated as linear. Therefore, the frequency ratio for two symmetrically injected signals needs to be kept reasonably near unity. Two phasor diagrams are presented in Fig. 6 with frequency equal to $\omega_1 = \omega_0 - \Delta\omega$ and $\omega_2 = \omega_0 + \Delta\omega$ separately.

In theory, at resonance, β_1 and β_2 should be equal to each other. The phase and amplitude of the corresponding small signal harmonic components are used to calculate the angle. The error between this two angle signals is used to identify the control direction of the *d*-axis current. However, this method is found to be hard to implement. First, the frequency of injected signal is calculated based on the accurate measurement of the main harmonic frequency. However, the operation frequency of the system is usually not fixed in the real time. Additional filters are required. Several PLLs, band pass filters are required for the angle detection procedure, making practical signal processing highly complicated.

4 Electronic stiffness perturbation method

The electronic stiffness perturbation algorithm is shown in Fig. 7. It is based on the low-frequency modulation of the *d*-axis current amplitude. This has a noticeable impact in the stroke signal as well as generated power. By using a band pass filter (BPF) in the DC-side, the resulting small perturbation envelope in DC-current can be extracted and multiplied by the perturbation signal. The result is integrated to produce a correction signal, which corrects the electronic stiffness and meet the maximum power condition.

Calling I_{per} the low-frequency perturbation amplitude in the d-axis current magnitude, the full *d*-axis current is expressed by

$$I_d(t) = (I_d + I_{\text{per}} \sin \omega_1 t) \sin \omega_o t \tag{12}$$

The presence of $I_{\text{per}} \neq 0$ causes a perturbation in the stiffness which produces a stiffness force term in time domain by

$$F_{\text{perturbation}} k_{v1} x(t) \sin(\omega_1 t) \tag{13}$$

where ω_1 is defined as frequency of the perturbation signal and the k_{v1} is the equivalent perturbation stiffness. According to (8), the time domain equation with perturbation signal injected are rewritten by

$$\begin{aligned} &mx''(t) + cx'(t) + (k + k_v + k_{v1}\sin(\omega_1 t))x(t) \\ &= F\cos(\omega_o t) - k_e I_q \cos(\omega_o t + \theta) \end{aligned} \tag{14}$$

From (14), the perturbation terms rendering the system non-autonomous is confirmed to be very small. This kind of the system is termed as weakly non-autonomous system. The rigorous mathematical analysis result is developed here. A heuristic explanation is presented, based on the assumption that the low-frequency modulation of the *d*-axis current amplitude translates into a modulation of the stroke amplitude. Three relevant cases are analysed: operation below resonance (insufficient d-axis current main amplitude), resonance conditions, and operation above resonance (excessive d-axis current main amplitude). Table 1 shows the parameters of the system that are used in the analysis.

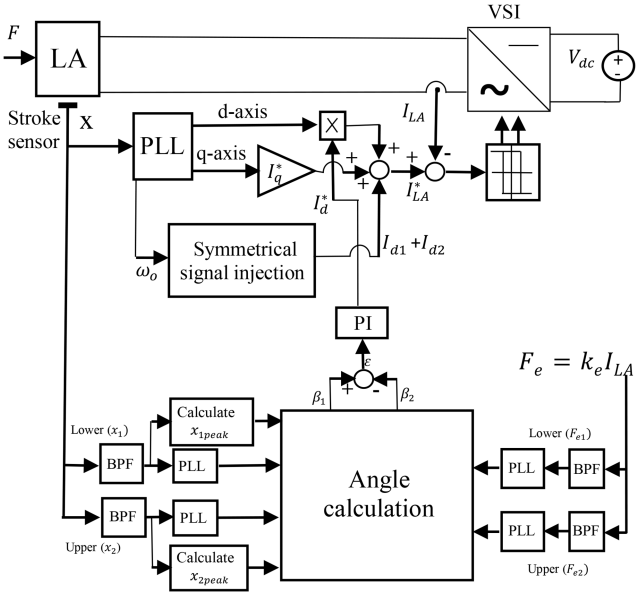

Fig. 5 *Symmetrical signal injection MPPT system schematic*

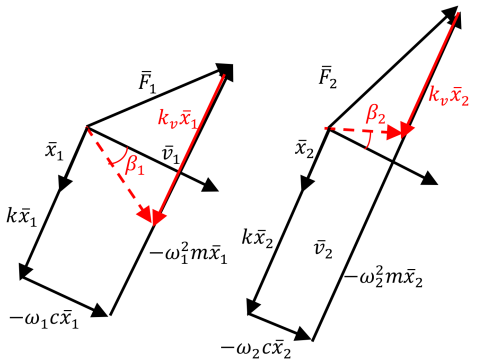

Fig. 6 *Phasor diagram for small symmetrical injected signals*

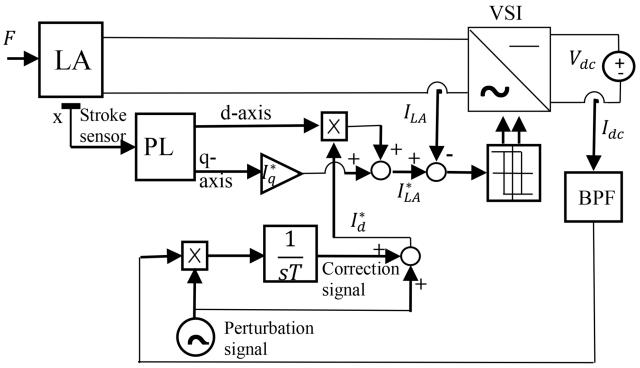

Fig. 7 *Electronic stiffness perturbation method schematic*

Table 1 System parameters

excitation force F = 600 N	spring stiffness k = 216539 N/m
LA plunger mass m = 2.194 kg	EMF constant K_e = 90 Vs/m
armature inductance L = 0.268 H	armature resistance R = 3.58 Ω
q-axis current I_q = 4 A	DC-side voltage V_{dc} = 1000 V

Fig. 8 presents the perturbation *d*-axis current amplitude and stroke envelope waveforms when insufficient *d*-axis current is applied. The I_{per} is divided by 100 to improve the readability of the plot. The operation frequency of the excitation force is set to 55 Hz with initial *d*-axis current set as zero. The equivalent perturbation stiffness is set as 10% of the spring mechanical stiffness in order to magnify the dynamic. ω_1 is 0.5 Hz. As seen from Fig. 8, the stroke envelope of x is in phase with perturbation *d*-axis current signal.

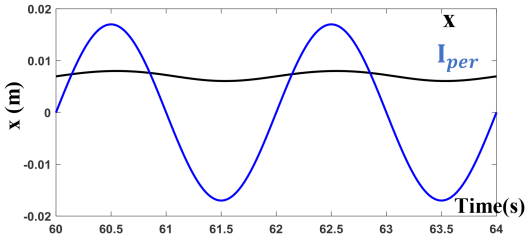

Fig. 8 *Stroke envelope and perturbation signals when insufficient d-axis current is applied*

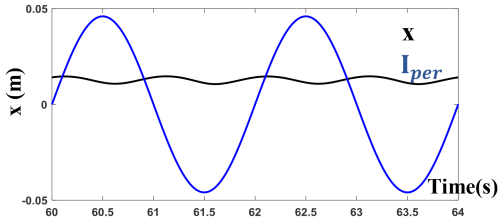

Fig. 9 *Stroke envelope and perturbation signals when system is in resonance*

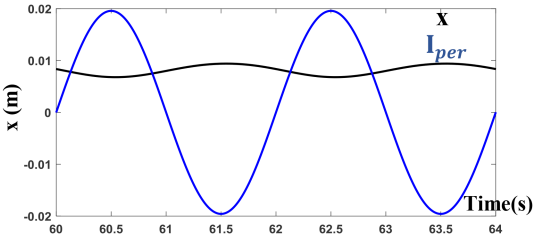

Fig. 10 *Stroke and perturbation signals when excessive Id is applied*

In theory, generated active power should have the similar envelope with the stroke from (5). As the DC-voltage is fixed, the envelope extracted from the moving average of the DCc-current should be in phase with the perturbation signal. This results in a mean positive value for the stiffness correction signal c_1, expressed as

$$c_1 = \int_0^{2\pi} A_1 I_{\text{per}} \sin(\omega_1 t)\sin(\omega_1 t) = A_1 I_{\text{per}}/2 \tag{15}$$

where A_1 is the amplitude of the extracted DC-current envelope. In Fig. 9, the operation frequency is set to be 50 Hz, which leads to resonance conditions for the system. As can be seen from Fig. 9, the frequency of the stroke envelope is now two times the frequency perturbation signal. This second harmonic will appear in the envelope of the DC-current moving average as well as in the generated active power, which then leads to a zero correction signal c_2.

$$c_2 = \int_0^{2\pi} A_2 I_{\text{per}} \sin(2\omega_1 t - \theta_1)\sin(\omega_1 t) = 0 \tag{16}$$

where θ_1 is the shifted phase produced because of BPF.

Fig. 10 presents the stroke and perturbation envelopes when excessive Id magnitude is applied. The frequency of the excitation force is set to 45 Hz. The envelope of the stroke is out of phase with the perturbation signal. The extracted envelope signal from the DC current will be out of phase with the perturbation signal as well.

The stiffness correction signal c_3 for excessive I_d is

$$c_3 = \int_0^{2\pi} -A_3 I_{\text{per}} \sin(\omega_1 t)\sin(\omega_1 t) = -A_3 I_{\text{per}}/2 \tag{17}$$

The perturbation signal used in this method is independent of the system operation frequency. This method is a direct control strategy as it uses the power information instead of position information to identify the control direction. Also, the signal detection stage is simple to implement as it only requires a band pass filter. Therefore, this strategy is chosen for the simulation.

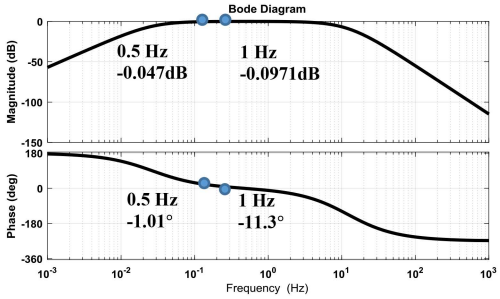

Fig. 11 *Bode plot of the band pass filter*

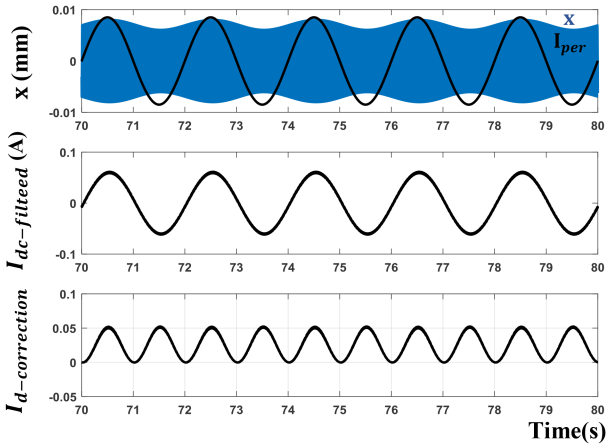

Fig. 12 *Stroke, perturbation signal, dc-current filtered signal and Id correction signal at system 55 Hz condition*

5 Simulation results

The I_d perturbation MPPT method is simulated by using Simulink with parameters in Table 1. The I_{per} needs to be carefully selected. An excessive amplitude will result in high stroke and power distortion. Conversely, a too small signal will make the signal processing challenging. For this reason, the equivalent perturbation stiffness is chosen as 5% of the mechanical stiffness. The ω_1 is set as 0.5 Hz. The I_d is set to zero initially within all simulations. The system operation frequency is modified to obtain required system. I_{per} is divided by 100 for comparison. A BPF is designed to extract a moving average from DC-current output. The BPF is designed to allow unity amplitude magnification with ω_1 and $2\omega_1$ signals with DC and high-frequency harmonic eliminated, from Fig. 11. The phase shift for the ω_1 signal is almost zero. For $2\omega_1$ signal, the phase shift will not affect the correction signal result as it is always equal to zero.

Fig. 12 presents steady-state waveforms when Id is not high enough. Subplots show perturbation, stroke, DC-current signal after filter $I_{\text{dc-filtered}}$ and correction signal $I_{\text{d-correction}}$. The operation frequency is 55 Hz. The main harmonic of the stroke is measured as 0.0071 m without I_d. The I_{per} is 0.85 A. The stroke is in phase with the perturbation signal as well as with the filtered DC-current signal. A positive correction for I_d follows. Waveforms in Fig. 13 refer to steady-state waveforms when system is in resonance. The main harmonic of the stroke is equal to 0.01273 m without I_d. The I_{per} is calculated as 1.5314 A. Low-frequency second-harmonic signal appears in the DC-current extracted signal (moving average): this results in a zero correction for I_d. Steady-state waveforms when I_d is too high are shown in Fig. 14. The system frequency is 45 Hz. The main harmonic of the stroke is 0.00814 m without I_d. I_{per} is 0.979 A. The stroke and filtered DC-current

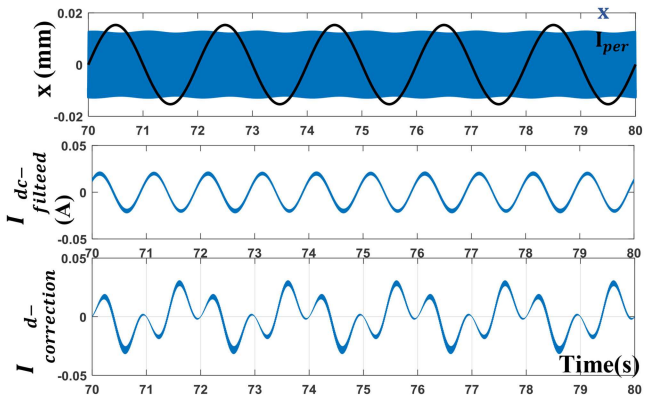

Fig. 13 *Stroke, perturbation signal, dc-current filtered signal and Id correction signal at system 50 Hz condition*

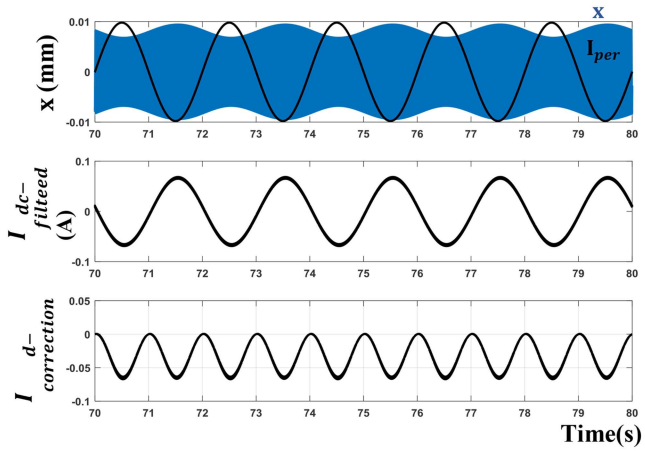

Fig. 14 *Stroke, perturbation signal, dc-current filtered signal and Id correction signal at system 45 Hz condition*

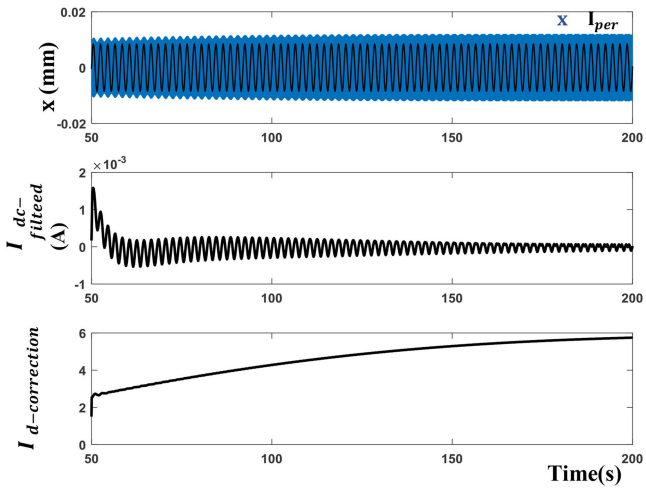

Fig. 15 *Stroke, perturbation signal, dc-current filtered signal and Id correction signal at system 55 Hz condition (closed loop)*

signal are out of phase with perturbation current signal. This leads to a negative correction for I_d.

A closed-loop result is provided in Fig. 15 to validate the control performance. Subplots comprise perturbation signal, stroke, current signal after BPF, and stiffness correction signal. The system frequency is 55 Hz and the LA resonant frequency is 50 Hz, so the system is initially out of resonance. The measured stroke would be 0.0118 m when system is in resonance at 55 Hz. The required additional stiffness would be 45473 N/m and from (6) the corresponding required Id* is 5.96 A. In Fig. 7, an integrator is used for integrating the correction signal to build the reference Id value. The integrator is started to be applied after 50 from the beginning of the simulation. The time coefficient T for the integrator is selected based on different scenarios. For instance, the wave input for WEC applications usually is modified frequently and this require a more quick response for MPPT loop. A small T is compulsory. Conversely, the frequency of the input pressure wave changes in a slow manner in TAE-LA applications. In this condition, a big T could be enough. The T is selected as 0.004 s in simulation. The Id* reference takes about 150 s to change from 0 to 5.94 A. This matched with the required Id* amount. The stroke is increased from 0.00707 to 0.0118 m until system is in resonance. By using (5), the generated active power is proved to increase by 40%.

6 Conclusion

The goal of this paper is to propose novel LA MPPT strategies by using a signal injection approach. Two methods have been proposed. The first one is based on the injection of two *d*-axis current signals at frequencies symmetrically shifted with respect to the operating frequency of the system. In principle, the analysis of the phase shifts in the corresponding harmonics in the stroke allows the resonance condition to be detected. The signal processing, however, appears to be extremely challenging. The second method is based on the low-frequency perturbation of the electronic stiffness, which is practically obtained by modulating at low frequency the amplitude of the main *d*-axis current. The low-frequency harmonic appearing in the stroke envelope allows in- and out-of-resonance conditions to be detected and the reactive current amplitude to be corrected accordingly. The preliminary simulation results confirm that this is a viable method, but a full analysis needs to be developed, particularly for the design of the adaptation mechanism.

7 References

[1] Park, J., Gu, B., Kim, J., *et al.*: 'Active phase control for maximum power point tracking of a linear wave generator', *IEEE Trans. Power Electron.*, 2016, **32**, pp. 7651–7662

[2] Vernaak, R., Kamper, M.J.: 'Experimental evaluation and predictive control of a air-cored linear generator for direct drive wave energy converters', *IEEE Trans. Ind. Appl.*, 2012, **48**, pp. 1817–1826

[3] Shek, J., Macpherson, D., Mueller, M., *et al.*: 'Reaction force control of a linear electrical generator for direct drive wave energy conversion', *IET Renew. Power Gener.*, 2007, **1**, pp. 17–24

[4] Wu, F., Zhang, X., Ju, P., *et al.*: 'Optimal control for AWS-based wave energy conversion systems', *IEEE Trans. Power Syst.*, 2009, **24**, pp. 1747–1755

[5] Zheng, P., Tong, C., Bai, J., *et al.*: 'Electromagnetic design and control strategy of an axially magnetized permanent-magnet linear alternator for free-piston stirling engines', *IEEE Trans. Ind. Appl.*, 2012, **48**, pp. 2230–2239

[6] Wang, T., Jiao, Z., Yan, L.: 'Resonant frequency recognition and tracking for linear oscillating motor under hydraulic load'. IEEE Int. Conf. on Aircraft Utility Systems (AUS), Beijing, China, 2016

[7] Amon, E., Brekken, T., Schacher, A.: 'Maximum power point tracking for ocean wave energy conversion', *IEEE Trans. Ind. Appl.*, 2012, **48**, pp. 1079–1086

[8] Tedeschi, E., Molinas, M.: 'Impact of control strategies on the rating of electric power take off for wave energy conversion'. 2010 IEEE Int. Symp. on Industrial Electronics (ISIE), Bari, Italy, 2010